Indian Journal of Heterocyclic Chemistry
Vol. 30 - Number 02 (Apr-Jun 2020) 189-196

ISSN (Print) : 0971-1627
ISSN (Online) : 2456-4311

2-Hydroxyethylammonium Mesylate Ionic Liquid Modified SBA-15/HEAM Silica Mesoporous: An Efficient Catalyst for the Preparation of Some New 2,4,6-Triarylpyridines under Solvent-free Approach

Mohammad Reza Asaadi[1]*, Hossein Behmadi[2], Abdolhossein Massoudi[1]

[1]Department of Chemistry, Faculty of Science, Payame Noor University, Tehran, Iran
[2]Department of Chemistry, Mashhad Branch, Islamic Azad University, Mashhad, Iran

ABSTRACT A new 2-hydroxyethylammonium mesylate ionic liquid (HEAM IL) was immobilized on SBA-15 as an efficient, green, and powerful catalyst for the preparation of new 4-aryl-2,6-di(pyren-1-yl)pyridines **(4a-f)** under mild and solvent-free reaction conditions. For this purpose, HEAM IL was first synthesized through the reaction between ethanolamine and methanesulfonic acid and then immobilized into the chloropropyl modified ordered mesochannels of SBA-15. After the successful characterization of the catalyst, the efficiency of SBA-15/HEAM was investigated in the one-pot three-component synthesis of 2,4,6-triaryl pyridine derivatives with 1- acetylpyrene, aryl aldehydes, and ammonium acetate under solvent-free conditions. This catalytic system was efficiently reused for nine consecutive runs.

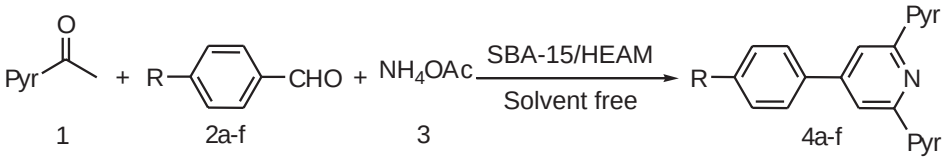

KEYWORDS 2-hydroxyethylammonium mesylate, 4-Aryl-2,6-di(pyren-1-yl)pyridines, Ionic liquid, Multicomponent reactions, SBA-15 silica mesoporous.

INTRODUCTION

In recent years, ionic liquids (ILs) possess unique and tunable properties for a wide array of applications. Due to the low vapor pressure, high electrochemical stability, low flammability, high intrinsic ionic conductivity, and tunable solubility for various materials, they have attracted huge academic and industrial interests.[1-3] Interestingly, the desirable properties of ILs could be attained by adjusting the chemical structure and functionality of their anions and cations and/or their appropriate mixing with other ILs and special solvents.[2,4,5] The various kind of ILs has been synthesized and used as a green replacement of common solvents or promising catalytic media in the modern synthesis of organic and inorganic compounds and other applications such as photochemistry, biotechnology, separation, fuel cells, electrolytes of batteries, and solar cells.[6-12] In general, ILs can be divided in two main categories according to their chemical properties: Protic ILs (PILs)[2] and aprotic ILs (AILs).[13] The chemical structure of AILs consists of bulky organic cations and diverse range of inorganic anions. Substituted imidazolines, alkyl pyridiniums, and trialkylamines as counter ions in the presence of inorganic anions were reported for AILs. The PILs are produced through reaction between appropriate Brønsted bases and Brønsted acids. Various substituted amines as cations and organic deprotonated acids as anions were used for the synthesis of PILs.[14] Furthermore, simple synthetic procedure and low cost of PILs are the useful advantages for large scale applications.[15] Various methods have been

*Corresponding author: Email: asadi.mreza1@gmail.com

Published & Hosted by :
Journal Homepage :
www.connectjournals.com/ijhc
www.connectjournals.com

reported for the synthesis of PILs with different anions and cations.[16,17] The anions of PILs have important roles in catalysis, absorption, biomass pretreatment, etc.[18-20] Based on literature, kinds of ILs have been used in multicomponent reactions (MCRs),[21] nitration reaction,[22] Diels–Alder reaction,[23] condensation reactions,[24] and etc.[25] However, the widespread use of ILs is affected by some disadvantages such as high viscosity, difficulty of isolation of the products, recovery, and handling of the catalyst. The use of diverse range of supports for immobilization of ILs can help to overcome these disadvantages. In this regard, a variety of supports have been introduced for the immobilization of ILs such as silica,[26] polymers,[27] carbon,[28] and magnetic materials.[29] The immobilization strategy can enhance the reactivity and selectivity of catalysts.[30-34]

Pyridine and its derivatives as important *N*-containing heterocycles found in different fields such as natural products and pharmaceuticals.[35] Among the pyridine family, Substituted Kröhnke pyridines (2,4,6-triarylpyridine derivatives) have been utilized as intermediates in the synthesis of therapeutic drugs, insecticides, herbicides, and surfactants,[36] chemosensors,[37] ligands,[38] and photosensitizers.[39] Various synthetic routes were reported for producing of these scaffolds which most of them relied on the catalyzed cyclocondensation of aldehydes, ketones, and ammonium salt as the nitrogen source.[40] The reaction of benzyl amines and ketones through oxidative cleavage of C–N bonds[41] and reaction of benzyl halides with acetophenone[42] were also reported for the synthesis of 2,4,6-triarylpyridines. MCR of acetophenones, benzaldehydes, and ammonium acetate as an important and effective pathway for the synthesis of 2,4,6-triarylpyridines was reported through ILs,[43] PEG1000-DAIL,[44] PFPAT,[45] MIL-101-SO_3H,[46] DPTA,[47] $ZrOCl_2$,[48] or TiO_2-SO_3H[49] catalyzed reactions. These methods encounter some drawbacks such as a large amount of catalyst, commercially unavailable catalysts, long reaction times with low yields and high reaction temperatures. Based on this knowledge, the development of simple and efficient catalytic procedures is still in demand.

In this paper, we report a convenient and facile one-pot procedure for the synthesis of aryl (pyren-1-yl) pyridine derivatives by the reaction of 1-acetylpyrene, aryl aldehydes, and ammonium acetate in solvent-free condition. Herein, we wish to introduce a new strategy for synthesis of a 2-hydroxyethyl ammonium mesylate modified SBA-15 silica mesoporous as a novel and recyclable heterogeneous catalyst. The catalytic activity of SBA-15/2-hydroxyethylammonium mesylate (HEAM) was studied for the preparation of aryl(pyren-1-yl)pyridine derivatives. The porous surface of SBA-15 was modified with 3-chloropropyltrimethoxysilan (CPTMS) groups, which was then converted to the 2-hydroxyethyl ammonium mesylate groups (**Scheme 1**).

RESULTS AND DISCUSSION

A new HEAM immobilized mesoporous SBA-15 catalyst was prepared. In the first step, SBA-15 with high surface area as porous support was synthesized. The synthesized SBA-15 was functionalized with CPTMS and then reacted with prepared HEAM to produce ILs functionalized SBA-15 (SBA-15/HEAM). The preparation steps of catalyst are shown in **Scheme 2**.

The CHNS elemental analysis was used to measure the content of carbon, nitrogen, and sulfur elements of catalyst which was presented in **Table 1**. The results confirm the elemental composition of immobilized organic moieties into the porous structure of catalyst. The amount of loaded HEAM ILs from carbon, nitrogen, and sulfur percent for final SBA-15/HEAM catalyst was calculated approximately 0.5 mmol/g. The nitrogen adsorption-desorption study was used for the textural analysis of catalyst (**Table 2**). The specific surface area, pore size, and pore volume of SBA-15, SBA-15/Cl, and SBA-15/HEAM samples were measured. The SBA-15 has a specific surface area of 835.5 m^2/g which was decreased to 712.3 and 546.6 m^2/g for SBA-15/Cl and SBA-15/HEAM, respectively. The observed trend confirms the immobilization of organic moieties into the porous structure of catalyst in each synthetic pathway. Furthermore, it is clear that the pore size and pore volume of the catalyst was decreased in each modification step. Based on these results, the pore volume of the final catalyst was 0.89 cm^3/g, which is sufficient for catalytic performance.

For the thermal stability study of nano-catalyst and calculation of the amount of ILs on the surface of SBA-15/HEAM, TGA was carried out in a static N_2 atmosphere (**Figure 1**). In the TGA curve of the final catalyst, different weight loss steps were observed in the temperature region of 30–800°C. Probably, the weight loss up to 150°C was due to the surface adsorbed water molecules (about 4 wt.%). About the 13 wt.% of weight loss was observed at 200–600°C which was attributed to the decomposition of surface organic groups of catalyst. These results are in good agreement with CHNS elemental analysis.

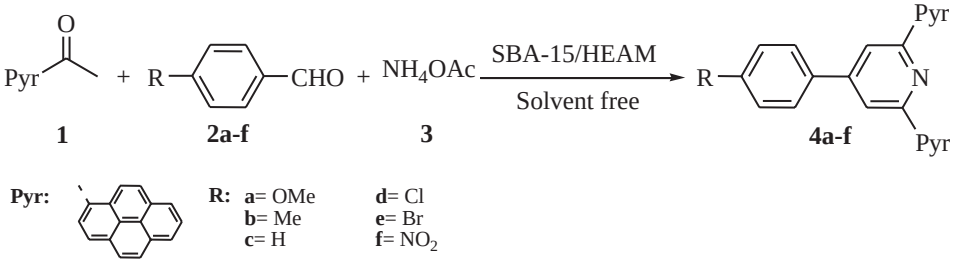

Scheme 1: SBA-15/2-hydroxyethylammonium mesylate catalyzed synthesis of 4-aryl-2,6-di(pyren-1-yl)pyridines (4a-f)

The chemical structure of SBA-15, SBA-15/Cl, and SBA-15/HEAM was studied by FT-IR spectrum (**Figure 2**). An intense absorption peak at 1100 cm^{-1} was attributed to the asymmetric vibration of Si-O-Si bonds in the FTIR of SBA-15 (**Figure 2a**). The characteristic symmetric stretching vibration peak of Si-OH bonds was observed as a small bond at about 955 cm^{-1} in the FTIR of SBA-15. The asymmetric vibration of SiO-H groups was observed in the 3000–3750 cm^{-1} region as a very broad absorption band. These results in comparison with literature confirm the successful synthesis of SBA-15 mesoporous. [33,34] The FTIR spectrum of SBA-15/Cl showed the characteristic peaks of SBA-15 with some changes (**Figure 2b**). The intensity of small Si-OH bonds and broad SiO-H bonds was decreased in the FTIR spectrum of SBA-15/Cl and SBA-15/HEAM (**Figure 2b and c**) in comparison with SBA-15 spectrum which is evidence for immobilization of mentioned organic groups. The asymmetric stretching vibration of aliphatic CH groups was appeared in the 2800–3000 cm^{-1} region (**Figure 2b**). In addition to the mentioned characteristic peaks, the FT-IR spectrum of SBA-15/HEAM showed the sharpening band around 2800–3600 cm^{-1} and 1020 due to the asymmetric stretching vibration of ammonium and sulfonic groups. The N–H plane bonding vibrations were appeared at 1600 cm^{-1}. Probably, the observed change in the intensity of vibrational peaks between 1100 and 1500 is due to the S=O and C-N stretching vibrations (**Figure 2c**).[50]

The TEM and SEM images were used for size and morphology study of SBA-15 and SBA-15/HEAM catalyst (**Figure 3**). A highly ordered mesoporous structure of SBA-15 was illustrated at TEM image of SBA-15 in **Figure 3a**. The presence of straight channels arraying along the long axis confirms the characteristic long-chain structure of SBA-15. The highly ordered mesopores arranged structure of SBA-15/HEAM was clearly observed in **Figure 3b**. **Figure 3** images confirm that the structural orderliness of bare SBA-15 is still retained after chemical immobilization of HEAM ILs. The SEM image of SBA-15/HEAM given in **Figure 3b** show consists of many worm-like domains which were referred to SBA-15 structure.[33]

After thorough characterization of the catalyst, catalytic performance of the SBA-15/HEAM as a IL-functionalized silica mesoporous catalyst was investigated to find the optimal reaction conditions in terms of the amount of catalyst, solvent, and temperature in the case of new 4-aryl-2,6-di(pyrene-1-yl)pyridine derivatives **4a-f (Scheme 1)**. The one-pot three-component reaction of 1-actylpyrene, benzaldehyde, and ammonium acetate was selected as a model reaction. The effect of reaction parameters and obtained experimental results in the case of model reaction is summarized in **Table 2**. The model reaction was examined without catalyst, with SBA-15 (50 mg) and SBA-15/HEAM (20 mg) in polar and non-polar solvents at reflux condition (**Table 2**, entries 1-9). The results showed that the corresponding product was produced in a significant 96% of yield in solvent-free conditions (**Table 1**, entries 10). The highest yield and shortest reaction time were achieved in the presence of 5 mg of SBA-15/HEAM at 60°C under solvent-free condition (**Table 2**, entry 13).

Subsequently, after the optimization of reaction conditions in the model reaction, the efficacy and applicability of SBA-15/HEAM as a IL functionalized SBA-15 catalyst in the preparation of new 4-aryl-2,6-di(pyrene-1-yl)pyridine derivatives were illustrated. Various arylaldehydes with electron-donating and electron-withdrawing groups were treated with 1-actylpyrene and ammonium acetate to furnish the corresponding products **4a-f** with high yields and short reaction times. The experimental data from this new protocol are summarized in **Table 3**.

All of the products were characterized by their melting points, FTIR, mass analysis, and NMR spectral and elemental analytical data. The recovery and reusability of the catalyst were also studied which is an important factor for industrial applications and green chemistry point of view. For this purpose, a set of experiments were tested to recover and reutilize the catalyst in the model reaction. After each catalytic cycle, the catalyst was easily filtered from the reaction mixture and washed 3 times with ethanol then dried at 60°C in the oven for 2 h. Next model reaction was started using the recovered catalyst and fresh substrates. This process was repeated for nine consecutive runs without a significant decrease of catalytic activity (**Figure 4**). The yield of the final product was decreased from 95% to 81%. The observed decrease in catalytic activity can be attributed to the catalyst poisoning which is caused by chemical compounds. Furthermore, leaching of the active ionic centers of catalyst in interaction with substrates causes the activity loss during the recyclability study of catalyst.

EXPERIMENTAL

Materials and apparatus

All starting materials and solvents were obtained from Merck and Sigma-Aldrich applied without additional purification. For morphology and size study, transmission electron microscopy (TEM) and scanning electron microscope (SEM) experiments were conducted on a Leo 912AB microscope operated at 120 kV and Leo 1450VP, respectively. The thermal stability and percentage weight loss of organic functionality were measured by thermal gravimetric analysis (TGA) (Mettler Toledo LF). Fourier-transform

Table 1: Elemental composition and nitrogen adsorption-desorption analysis of the catalyst

Sample	C^a (wt%)	N^a (wt%)	S^a (wt%)	$S_{BET}{}^b$ (m^2/g)	d^c (nm)	V^d (cm^3/g)
SBA-15	-	-	-	835.5	6.4	1.78
SBA-15/Cl	5.1	-	-	412.3	5.7	1.21
SBA-15/HEAM	11.2	4.4	2.3	546.6	4.5	0.89

[a]Based on CHNS analysis, [b]Surface area, [c]Pore size, [d]Pore volume. HEAM: 2-hydroxyethylammonium mesylate

infrared (FT-IR) spectra were collected on a Bruker Tensor 27 spectrometer on KBr discs. ^{1}H and ^{13}C nuclear magnetic resonance (NMR) spectra were measured on a Bruker 300 DRX Avance instrument using DMSO-$d_6$as solvent and tetramethylsilane as an internal standard. Elemental analysis was performed on a Thermo Finnigan Flash EA microanalyzer. Melting points were measured on Stuart SMP3 apparatus.

Preparation of HEAM

In a 500 mL round-bottomed flask equipped with a dropping funnel, 200 mL methanol as the solvent and 0.1 mol of methanesulfonic acid were mixed and then 0.1 mol monoethanolamine solution was added drop by drop in the ice bath stirring. The reaction mixture was stirred at room temperature for 24 h. Then, the solvent was removed and the final HEAM was obtained which was dried out in a vacuum drying oven.

Procedure for construction of SBA-15 mesoporous

Ordered silica mesoporous (SBA-15) was prepared according to the previously reported procedure.[33] 2.0 g of pluronic P123 and 15 g of ultrapure water were stirred at room temperature and 60 g aqueous solution of HCl (2 M) was added and stirred for 30 min. In the next step, 4.25 g of tetraethyl orthosilicate was added to the above solution and reacted for 20 h. Then, the mixture was aged at 80°C for 24 h. The final white powder was filtered and washed with water before calcination at 500°C for 6 h (heating rate of 1°C.min^{-1}).

Procedure for construction of SBA-15/HEAM

One gram of activated SBA-15 was dispersed in 30 mL of dry toluene and 1 mmol of CPTMS was added drop by drop before refluxing at 110°C for 6 h. The white powder named SBA-15/Cl was filtered and washed with toluene and ethyl acetate 3 times. In the final step, 1.5 mmol of HEAM and 1 g of SBA-15/Cl were dispersed with ultrasonic in dry toluene for 60 min. The resulting mixture was heated at 60°C for 12 h. Soxhlet extraction in dry toluene was performed for removal of residual organic moieties. The white solid named SBA-15/HEAM dried in oven at 60°C for 2 h.

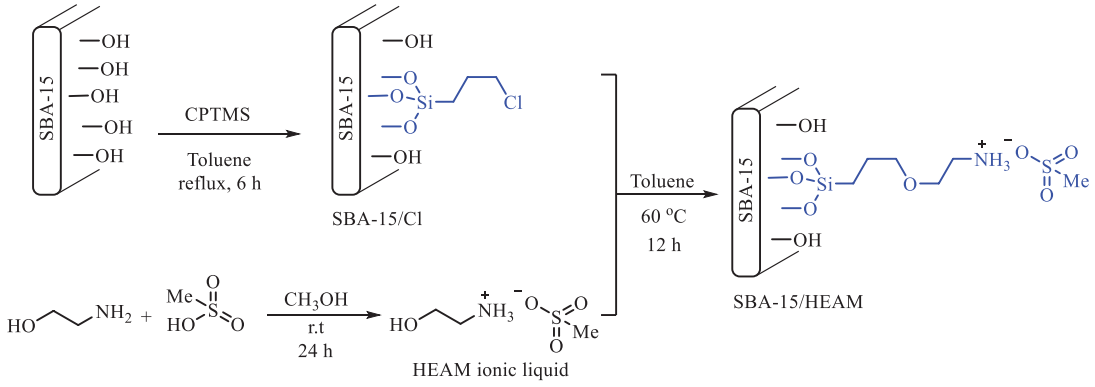

Scheme 2: Preparation of SBA-15/2-hydroxyethylammonium mesylate

Table 2: Optimization of the reaction conditions for the synthesis of 2,4,6-triarylpyridine derivative 4c[a]

Entry	Catalyst	Catalyst amount (mg)	Solvent	Temperature (°C)	Time (min)	Yield (%)[b]
1	-	-	H_2O	reflux	500	10
2	SBA-15	50	H_2O	reflux	300	30
3	SBA-15/HEAM	20	H_2O	reflux	80	85
4	SBA-15/HEAM	20	DMSO	reflux	90	85
5	SBA-15/HEAM	20	DMF	reflux	100	75
6	SBA-15/HEAM	20	EtOH	reflux	80	80
7	SBA-15/HEAM	20	H_2O/EtOH	reflux	100	80
8	SBA-15/HEAM	20	n-hexane	reflux	400	trace
9	SBA-15/HEAM	20	CH_2Cl_2	reflux	400	trace
10	SBA-15/HEAM	20	-	100	80	96
11	SBA-15/HEAM	10	-	80	80	96
12	SBA-15/HEAM	10	-	60	80	96
13	**SBA-15/HEAM**	**5**	**-**	**60**	**80**	**95**
14	SBA-15/HEAM	5	-	r.t	400	-

[a]Reaction conditions: benzaldehyde (1 mmol), 1-actylpyrene (2 mmol), ammonium acetate (1.5 mmol) and catalyst (x mg). [b]Isolated yields.
HEAM: 2-hydroxyethylammonium mesylate

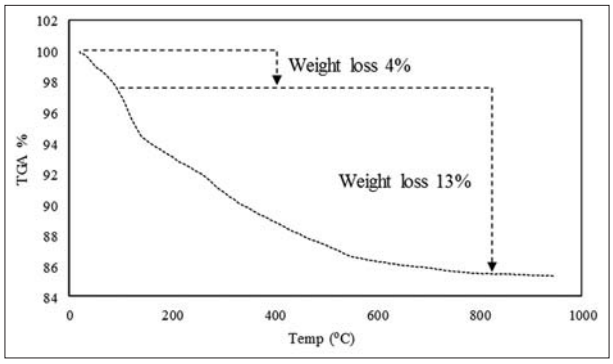

Figure 1: Thermogravimetric analysis curve of SBA-15/2-hydroxyethylammonium mesylate

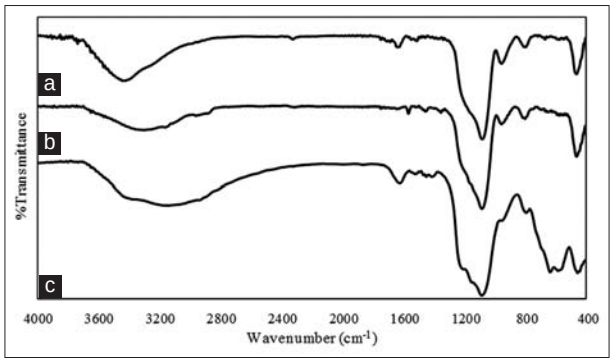

Figure 2: Fourier-transform infrared of (a) SBA-15, (b) SBA-15/Cl, (c) SBA-15/2-hydroxyethylammonium mesylate

General procedure for synthesis of 4-aryl-2,6-di(pyren-1-yl)pyridines(4a-f)

In a test tube, 1- acetylpyrene **1 (**2 mmol), aryl aldehyde **2a-f** (1 mmol), ammonium acetate **3 (**2 mmol), and 5 mg of SBA-15/HEAM catalyst were mixed, under stirring with a magnetic stirrer, the obtained reaction mixture was heated at 60°C in solvent-free conditions for appropriate times (**Table 3**). After the completion of the reaction (monitored by thin-layer chromatography using a mixture of n-hexane and ethyl acetate as eluent), 10 mL hot DMSO was added to the mixture and catalyst was separated from the reaction mixture by simple filtration and washed 3 times with ethanol and recovered for subsequent reaction. The crude product was recrystallized from DMSO to give pure compounds **4a-f**.

Characterization data

4-(4-Methoxyphenyl)-2,6-di(pyren-1-yl)pyridine ***(4a)***

Yield 68%, brown powder, mp 140–143°C, IR spectrum, *v*, cm^{-1}: 3038 (arom-CH), 1593, 1514, 1249, 1178, 1032, 840; ^1H NMR spectrum (DMSO-d_6), δ, ppm (J, Hz): 3.85 (s, 3H, OCH_3), 7.11–8.68 (m, 12H, arom-H); ^{13}C NMR (DMSO-d_6), δ, ppm: 55.80, 115.15, 121.42, 124.45, 124.68, 125.39, 125.68, 126.04, 126.91, 127.85, 128.45, 128.63, 129.22, 129.93, 130.82, 131.38, 131.41, 136.23, 148.89, 159.65, 160.97; Mass spectrum (EI, 70 eV), *m/z*: 585.2 $[M]^+$; Found, %: C 89.18; H 4.38; N 2.31. $C_{44}H_{27}NO$. Calculated, %: C 90.23; H 4.65; N 2.39; O 2.73.

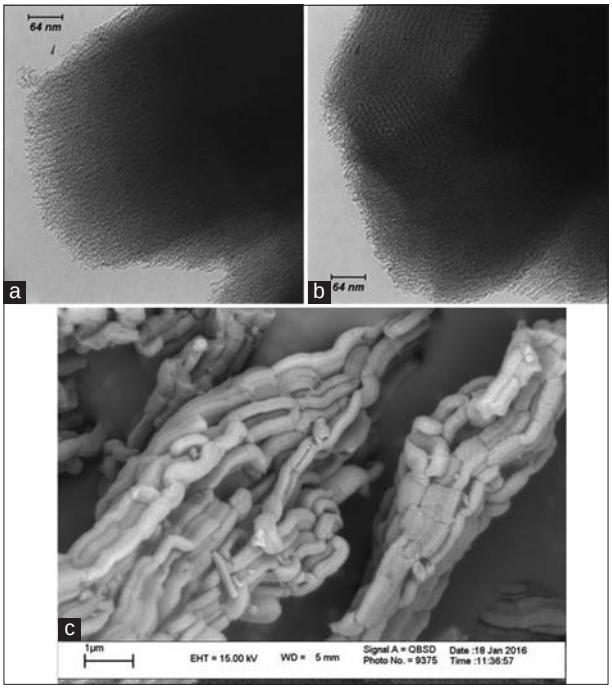

Figure 3: TEM image of (a) SBA-15, (b) SBA-15/2-hydroxyethylammonium mesylate (HEAM) and SEM image of (c) SBA-15/HEAM

2,6-Di(pyren-1-yl)-4-p-tolylpyridine ***(4b)***

Yield 65%, brown powder, mp 129–131°C, IR spectrum, *v*, cm^{-1}: 3038 (arom-CH), 1591, 1535, 1393, 1185, 842; ^1H NMR spectrum (DMSO-d_6), δ, ppm (J, Hz): 2.41 (s, 3H, CH_3), 7.39–8.69 (m, 12H, arom-H); ^{13}C NMR (DMSO-d_6), δ, ppm: 21.18, 119.27, 122.49, 124.17, 124.38, 125.80, 126.59, 126.76, 127.31, 127.66, 129.57, 130.69, 132.77, 132.92, 133.18, 139.01, 139.70, 149.95, 159.02; Mass spectrum (EI, 70 eV), *m/z*: 569.2$[M]^+$; Found, %: C90.08; H4.53; N2.36. $C_{44}H_{27}N$. Calculated, %: C 92.76; H 4.78; N 2.46.

4-Phenyl-2,6-di(pyren-1-yl)pyridine ***(4c)***

Yield 79%, light green powder, mp 199–202°C, IR spectrum, *v*, cm^{-1}: 3036 (arom-CH), 1589, 1538, 1396, 840, 757, 716; ^1H NMR spectrum (DMSO-d_6), δ, ppm (J, Hz): 7.56-8.71 (m, 10H, arom-H); ^{13}C NMR (DMSO-d_6), δ, ppm: 122.10, 124.46, 124.70, 125.41, 125.70, 126.07, 126.93, 127.85, 127.94, 128.43, 128.52, 128.64, 129.76, 129.96, 130.83, 131.39, 131.47, 136.08, 137.94, 149.43, 159.76; Mass spectrum (EI, 70 eV), *m/z*: 555.1$[M]^+$; Found, %: C90.87; H4.46; N 2.45. $C_{43}H_{25}N$. Calculated, %: C 92.94; H 4.53; N 2.52.

4-(4-Chlorophenyl)-2,6-di(pyren-1-yl)pyridine ***(4d)***

Yield 82%, yellow powder, mp 160–163°C, IR spectrum, *v*, cm^{-1}: 3041(arom-CH), 1593, 1537, 1493, 1386, 1093, 838; ^1H NMR spectrum (DMSO-d_6), δ, ppm (J, Hz): 7.62–8.69 (m, 12H, arom-H); ^{13}C NMR (DMSO-d_6), δ, ppm: 121.95, 124.42, 124.67, 125.38, 125.70, 126.07, 126.92, 127.83, 128.44, 128.51, 128.63, 128.68, 129.67, 129.77, 130.80, 131.36, 131.48, 134.89, 135.93, 136.69, 148.10, 159.81; Mass spectrum (EI, 70 eV), *m/z*: 589.1$[M]^+$; Found, %: C86.14; H3.97; N 2.29. $C_{43}H_{24}ClN$. Calculated, %: C 87.52; H 4.10; Cl 6.01; N 2.37.

Table 3: One-pot synthesis of 4-aryl-2,6-di(pyrene-1-yl)pyridine derivatives (4a-f) according to Scheme 1

Entry	Product	R	Time (min)	Yield (%)[b]
1	**4a**	OMe	90	90
2	**4b**	Me	90	90
3	**4c**	H	80	95
4	**4d**	Cl	75	92
5	**4e**	Br	75	90
6	**4f**	NO_2	70	95

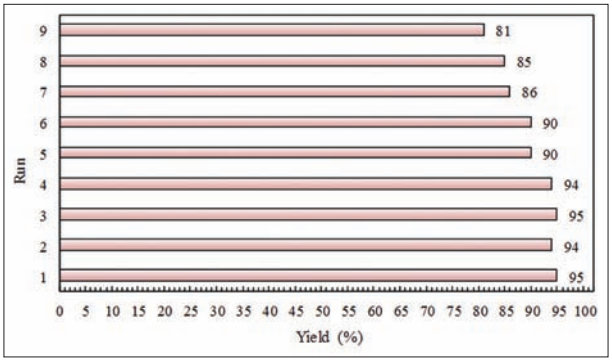

Figure 4: Recyclability of the catalyst in the model reaction

4-(4-Bromophenyl)-2,6-di(pyren-1-yl)pyridine ***(4e)***

Yield 86%, orang powder, mp 217–219°C, IR spectrum, *v*, cm^{-1}: 3037 (arom-CH), 1592, 1536, 1490, 1380, 1011, 837; ^1H NMR spectrum (DMSO-d_6), δ, ppm (J, Hz): 7.77–8.69 (m, 12H, arom- H); ^{13}C NMR (DMSO-d_6), δ, ppm: 121.93, 123.64, 124.42, 124.66, 125.40, 125.73, 126.10, 126.96, 127.85, 128.16,128.47, 128.54, 128.63, 128.70, 130.09, 130.81, 131.26, 131.37, 131.49, 132.42, 132.63, 135.93, 137.10, 148.21, 159.84; Mass spectrum (EI, 70 eV), *m/z*: 633.1$[M]^+$; Found, %: C80.24; H3.75; N 2.13. $C_{43}H_{24}BrN$. Calculated, %: C 81.39; H 3.81; Br 12.59; N 2.21.

4-(4-Nitrophenyl)-2,6-di(pyren-1-yl)pyridine ***(4f)***

Yield 72%, dark green powder, mp 206–209°C, IR spectrum, *v*, cm^{-1}: 3043 (arom-CH), 1590, 1520, 1344, 1112, 846; ^1H NMR spectrum (DMSO-d_6), δ, ppm: 7.82–8.71 (m, 12H, arom- H); ^{13}C NMR (DMSO-d_6), δ, ppm: 117.23, 119.29, 122.47, 124.20, 124.41, 125.38, 125.76, 126.63, 126.81, 127.66, 130.69, 132.77, 132.92, 133.20, 138.98, 140.43, 149.82, 159.15; Mass spectrum (EI, 70 eV), *m/z*: 600.1$[M]^+$; Found, %: C84.88; H3.95; N 4.53. $C_{43}H_{24}N_2O_2$. Calculated, %: C 85.98; H 4.03; N 4.66; O 5.33.

CONCLUSIONS

In summary, the HEAM IL was prepared and successfully immobilized into the modified surface of SBA-15 mesoporous silica. The catalytic applicability of prepared SBA-15/HEAM was explored in the construction of new 4-aryl-2,6-di(pyren-1-yl)pyridinesunder mild and solvent-free reaction conditions. All of the desired pyridine derivatives were produced in high yields 90–95% and short reaction time (70–90 min) at 60°C which indicates the high catalytic activity of this catalyst.

ACKNOWLEDGMENT

The authors express their gratitude to the Payame Noor University, Mashhad Branch, for its financial support.

REFERENCES

[1] Hajipour, A.R., Rafiee, F. Recent progress in ionic liquids and their applications in organic synthesis, *Org. Prep. Proced. Int*., **2015**, *47*, 249–308.

[2] Greaves, T.L., Drummond, C.J. Protic ionic liquids: Evolving structure-property relationships and expanding applications, *Chem. Rev*., **2015**, *115*, 11379–11448.

[3] Miran, M.S., Hoque, M., Yasuda, T., Tsuzuki, S., Ueno, K., Watanabe, M. Key factor governing the physicochemical properties and extent of proton transfer in protic ionic liquids: ΔpKa or chemical structure? *Phys. Chem. Chem. Phys*., **2018**, *21*, 418–426.

[4] Vekariya, R.L. A review of ionic liquids: Applications toward scatalytic organic transformations, *J. Mol. Liq*., **2017**, *227*, 44–60.

[5] Khashavar, G. A review of ionic liquids, their limits and applications, *Green Sustain. Chem*., **2014**, *4*, 44–53.

[6] Amarasekara, A.S. Acidic ionic liquids, *Chem. Rev.*, **2016**, *116*, 6133–6183.

[7] Amde, M., Liu, J.F., Pang, L. Environmental application, fate, effects, and concerns of ionic liquids: A review, *Environ. Sci. Technol*., **2015**, *49*, 12611–12627.

[8] Dai, C., Zhang, J., Huang, C., Lei, Z. Ionic liquids in selective oxidation: Catalysts and solvents, *Chem. Rev*., **2017**, *117*, 6929–6983.

[9] Fabry, D.C., Ronge, M.A., Rueping, M. Immobilization and continuous recycling of photoredox catalysts in ionic liquids for applications in batch reactions and flow systems: Catalytic alkene isomerization by using visible light, *Chem. Eur. J*., **2015**, *21*, 5350–5354.

[10] Itoh, T. Ionic liquids as tool to improve enzymatic organic synthesis, *Chem. Rev.*, **2017**, *117*, 10567–10607.

[11] Dai, Z., Noble, R.D., Gin, D.L., Zhang, X., Deng, L. Combination of ionic liquids with membrane technology: A new approach for CO_2 separation, *J. Memb. Sci*., **2016**, *497*, 1-20.

[12] MacFarlane, D.R., Forsyth, M., Howlett, P.C., Kar, M., Passerini, S., Pringle, J.M., Zhang, S. Ionic liquids and their solid-state analogues as materials for energy generation and storage, *Nat. Rev. Mater*., **2016**, *1*, 15005.

[13] Reid, J.E., Prydderch, H., Spulak, M., Shimizu, S., Walker, A.J., Gathergood, N. Green profiling of aprotic versus protic ionic liquids: Synthesis and microbial toxicity of analogous structures, *Sustain. Chem. Pharm*., **2018**, *7*, 17-26.

[14] Vogl, T., Goodrich, P., Jacquemin, J., Passerini, S., Balducci, A. The influence of cation structure on the

chemical-physical properties of protic ionic liquids, *J. Phys. Chem. C*., **2016**, *120*, 8525–8533.

[15] Sun, J., Konda, N.V.S., Parthasarathi, R., Dutta, T., Valiev, M., Xu, F., Simmons, B.A., Singh, S. One-pot integrated biofuel production using low-cost biocompatibleprotic ionic liquids, *Green Chem*., **2017**, *19*, 3152–3163.

[16] Ullah, Z., Bustam, M.A., Man, Z., Muhammad, N., Khan, A.S. Synthesis, characterization and the effect of temperature on different physicochemical properties of protic ionic liquids, *RSC Adv*., **2015**, *5*, 71449–71461.

[17] Pin, T.C., Nakasu, P.Y., Mattedi, S., Rabelo, S.C., Costa, A.C. Screening of protic ionic liquids for sugarcane bagasse pretreatment, *Fuel*, **2019**, *235*, 1506–1514.

[18] Latos, P., Culkin, A., Barteczko, N., Boncel, S., Jurczyk, S., Brown, L.C., Nockemann, P., Chrobok, A., Swadźba-Kwaśny, M. Water-tolerant trifloaluminate ionic liquids: New and uniquelewis acidic catalysts for the synthesis of chromane, *Front. Chem*., **2018**, *6*, 535.

[19] Ren, S., Hou, Y., Zhang, K., Wu, W. Ionic liquids: Functionalization and absorption of SO_2, *Green Energy Environ*., **2018**, *3*, 179–190.

[20] Steinrueck, H.P., Wasserscheid, P. Ionic liquids in catalysis, *Catal. Lett*., **2015**, *145*, 380–397.

[21] Melo, L.R., Silva, W.A. Ionic liquid in multicomponent reactions: A brief review, *Curr. Green Chem*., **2016**, *3*, 120–132.

[22] Kar, B., Ghosh, P., Kundu, K., Bardhan, S., Paul, B.K., Das, S. Benzimidazolium-based high temperature ionic liquid-in-oil microemulsion for regioselective nitration reaction, *J. Mol. Liq*., **2018**, *268*, 122–130.

[23] Janus, E., Gano, M., Feder-Kubis, J., Sośnicki, J. Chiral protic imidazolium salts with a (-)-menthol fragment in the cation: Synthesis, properties and use in the Diels-Alder reaction, *RSC Adv*., **2018**, *8*, 10318–10331.

[24] Yao, N., Wu, Y.P., Zheng, K.B., Hu, Y.L. Recent advances in catalytic condensation reactions applications of supported ionic liquids, *Curr. Org. Chem*., **2018**, *22*, 462–484.

[25] Welton, T. Ionic liquids: A brief history, *Biophys. Rev*., **2018**, *10*, 691–706.

[26] Giacalone, F., Gruttadauria, M. Covalently supported ionic liquid phases: An advanced class of recyclable catalytic systems, *ChemCatChem*, **2016**, *8*, 664–684.

[27] Tomé, L.C., Gouveia, A.S., Freire, C.S., Mecerreyes, D., Marrucho, I.M. Polymeric ionic liquid-based membranes: Influence of polycation variation on gas transport and CO_2 selectivity properties, *J. Memb. Sci*., **2015**, *486*, 40–48.

[28] Zhang, H., Zhang, Q., Zhang, L., Pei, T., Dong, L., Zhou, P., Xia, L. Acidic polymeric ionic liquids based reduced graphene oxide: An efficient and rewriteable catalyst for oxidative desulfurization, *Chem. Eng. J*., **2018**, *334*, 285–295.

[29] Xie, W., Wan, F. Basic ionic liquid functionalized magnetically responsive Fe_3O_4@ HKUST-1 composites used for biodiesel production, *Fuel*, **2018**, *220*, 248–256.

[30] Lamei, K., Eshghi, H., Bakavoli, M., Rostamnia, S. Magnetically recoverable gold nanorods as a novel catalyst for the facile reduction of nitroarenes under aqueous conditions, *Catal. Lett*., **2017**, *147*, 491–501.

[31] Lamei, K., Eshghi, H., Bakavoli, M., Rostamnia, S. Highly dispersed copper/ppm palladium nanoparticles as novel magnetically recoverable catalyst for Suzuki reaction under aqueous conditions at room temperature, *Appl. Organomet. Chem*., **2017**, *31*, e3743.

[32] Hashemi, A.N., Eshghi, H., Lamei, K. Uniform silver nanoparticles on tunable porous N-doped carbon nanospheres for aerobic oxidative synthesis of aryl nitriles from benzylic alcohols, *Appl. Organomet. Chem*., **2019**, *33*, e4835.

[33] Rostamnia, S., Lamei, K., Pourhassan, F. Generation of uniform and small particle size of palladium onto the SH-decorated SBA-15 pore-walls: SBA-15/(SH) XPd-NPY as a recoverable nanocatalyst for Suzuki-Miyaura coupling reaction in air and water, *RSC Adv*., **2014**, *4*, 59626–59631.

[34] Rostamnia, S., Xin, H., Liu, X., Lamei, K. Simultaneously application of SBA-15 sulfonic acid nanoreactor and ultrasonic irradiation as a very useful novel combined catalytic system: An ultra-fast, selective, reusable and waste-free green approach, *J. Mol. Catal. A. Chem*., **2013**, *374*, 85–93.

[35] Scriven, E.F. *Pyridines*: *From Lab to Production*, Academic Press, United States, **2013**.

[36] Doebelin, C., Wagner, P., Bihel, F., Humbert, N., Kenfack, C.A., Mely, Y., Schmitt, M. Fully regiocontrolled polyarylation of pyridine, *J. Org. Chem*., **2014**, *79*, 908–918.

[37] Fang, A.G., Mello, J.V., Finney, N.S. Structural studies of biarylpyridines fluorophores lead to the identification of promising long wavelength emitters for use in fluorescent chemosensors, *Tetrahedron*, **2004**, *60*, 11075–11087.

[38] Aroua, S., Todorova, T.K., Hommes, P., Chamoreau, L.M., Reissig, H.U., Mougel, V., Fontecave, M. Synthesis, characterization, and DFT analysis of bis-terpyridyl-based molecular cobalt complexes, *Inorg. Chem*., **2017**, *56*, 5930–5940.

[39] Tsuji, Y., Yamamoto, K., Yamauchi, K., Sakai, K. Near-infrared light-driven hydrogen evolution from water using a polypyridyl triruthenium photosensitizer, *Angew. Chem. Int. Ed. Engl*., **2018**, *57*, 208–212.

[40] Zolfigol, M.A., Karimi, F., Yarie, M., Torabi, M. Catalytic application of sulfonic acid-functionalized titana-coated magnetic nanoparticles for the preparation of 1, 8-dioxodecahydroacridines and 2, 4, 6-triarylpyridines via anomeric-based oxidation, *Appl. Organomet. Chem*., **2018**, *32*, e4063.

[41] Gopalaiah, K., Rao, D.C., Mahiya, K., Tiwari, A. Iron-catalyzed aerobic oxidative cleavage and construction of C-N bonds: A facile method for synthesis of 2, 4, 6-trisubstituted pyridines, *Asian J. Org. Chem*., **2018**, *7*, 1872–1881.

[42] Adib, M., Ayashi, N., Mirzaei, P. An efficient synthesis of 2, 4, 6-triarylpyridines by use of benzyl halides under neat conditions, *Synlett*, **2016**, *27*, 417–421.

[43] Satasia, S.P., Kalaria, P.N., Raval, D.K. Acidic ionic liquid immobilized on cellulose: An efficient and recyclable heterogeneous catalyst for the solvent-free synthesis of hydroxylatedtrisubstituted pyridines, *RSC Adv*., **2013**, *3*, 3184–3188.

[44] Ren, Y.M., Zhang, Z., Jin, S. Convenient and efficient method for synthesis of 2, 4, 6-triarylpyridines using catalytic amount of PEG1000-based dicationic acidic ionic liquid under solvent-free conditions, *Synth. Commun*., **2016**, *46*, 528–535.

[45] Montazeri, N., Mahjoob, S. Highly efficient and easy synthesis of 2, 4, 6-triarylpyridines catalyzed by pentafluorophenylammonium triflate (PFPAT) as a new recyclable solid acid catalyst in solvent-free conditions, *Chin. Chem. Lett*., **2012**, *23*, 419–422.

[46] Boroujeni, M.B., Hashemzadeh, A., Faroughi, M.T., Shaabani, A., Amini, M.M. Magnetic MIL-101-SO_3H: A highly efficient bifunctional nanocatalyst for the synthesis of 1, 3, 5-triarylbenzenes and 2, 4, 6-triaryl pyridines, *RSC Adv*., **2016**, *6*, 100195–100202.

[47] Li, J., He, P., Yu, C. DPTA-catalyzed one-pot regioselective synthesis of polysubstituted pyridines and 1, 4-dihydropyridines, *Tetrahedron*, **2012**, *68*, 4138–4144.

[48] Moosavi-Zare, A.R., Zolfigol, M.A., Farahmand, S., Zare, A., Pourali, A.R., Ayazi-Nasrabadi, R. Synthesis of 2, 4, 6-triarylpyridines using $ZrOCl_2$ under solvent-free conditions, *Synlett*, **2014**, *25*, 193–196.

[49] Tabrizian, E., Amoozadeh, A., Rahmani, S., Imanifar, E., Azhari, S., Malmir, M. One-pot, solvent-free and efficient synthesis of 2, 4, 6-triarylpyridines catalyzed by nano-titania-supported sulfonic acid as a novel heterogeneous nanocatalyst, *Chin. Chem. Lett*., **2015**, *26*, 1278–1282.

[50] Cai, G., Yang, S., Zhou, Q., Liu, L., Lu, X., Xu, J., Zhang, S. Physicochemical properties of various 2-hydroxyethylammonium sulfonate-based protic ionic liquids and their potential application in hydrodeoxygenation, *Front. Chem*., **2019**, *7*, 196.

Received: 17 Dec 2019; Accepted: 06 Mar 2020